

Influences of changing sea ice and snow thicknesses on Arctic winter heat fluxes

Supplemental Material

5 Simulated winter Arctic surface heat fluxes with specified constant sea ice thicknesses

Atmosphere-only models that include sea ice concentration changes but fix sea ice thicknesses at a constant value will have inaccurate estimates for changes in surface heat fluxes (and thus also temperatures) in a warming world. For example, changes in conductive heat fluxes from a “typical” 20th Century mid-Arctic ocean (2./0.1 m thick sea ice/snow, ΔT of 40°) will be roughly halved/doubled with 20° warming depending on whether SIT and snow thicknesses are held constant, or thin to 10 0.5/0.02 m (sea ice/snow) (e.g. Supplemental Table 1). Changes in net surface heat fluxes (which are equal to conductive heat fluxes over ice-covered areas) and surface temperatures in CESM2 PAMIP (100 member ensembles) and AMIP (10-member ensembles) simulations show that while net surface heat fluxes increase outside of sea ice covered areas, they decrease over sea ice covered areas as the surface temperatures warm (Supplemental Fig. 1). For reference, Arctic sea ice volume decreased by ~66% from the mid-twentieth century to the present (Kwok, 2018; Lindsay and Schweiger, 2015). Thus, keeping SIT 15 constant during this period is in contrast to observations and will artificially introduce errors in surface heat fluxes – and therefore temperature changes over sea ice covered regions. The PAMIP experiments and protocols are further described by Smith et al., 2019. The CESM2 is further described in Simpson et al. (2020) and the AMIP-style runs SST and SIC boundary conditions are described in Hurrell et al. (2008).

CESM1-CICE vs 0-layer model

20 We explore the influence of sub-grid scale heterogeneity in sea ice and snow fields on conductive heat fluxes by using the Semnter 0-layer model to calculate conductive heat fluxes from daily grid-cell mean sea ice and snow thicknesses and surface temperatures, and then compute monthly averages to compare with the conductive heat fluxes from the model. Sea ice thermodynamics in the CESM1 are calculated for each of the five discrete ice thickness categories using the multi-layer thermodynamic scheme of Bitz and Lipscomb (1999; “CESM1-CICE”) which includes the effects of a prescribed vertical 25 salinity profile and time-evolving vertical temperature profile – a more complete and yet more complex calculation than the Semnter 0-layer model. Differences between the conductive heat fluxes calculated from the grid-cell mean variables and the model output will be due to differences in the thermodynamic models (Semnter and CESM1-CICE) as well as differences due to thickness distributions.

30 We assess how well the 0-layer model of Semtner estimates conductive heat fluxes compared to CESM1-CICE by evaluating
 daily output from three 30-member CESM1 ensembles that were run for 2-year time slices (1980-1981; 2021-2022; and 2051-
 2052) using the same forcing as the CESM1-LE (hereafter referred to as the CESM1-TS; DuVivier et al., 2020). These
 experiments – unlike the CESM1-LE – included daily output of ice and snow thicknesses in each of the five discrete thickness
 35 categories, enabling us to compare conductive heat fluxes calculated using the ice thickness distribution (ITD) and the 0-layer
 model to the climate model output. Daily grid-cell mean surface temperatures were used as neither the CESM1-LE nor the
 CESM1-TS output sub-gridcell surface temperature information. Furthermore, the CESM1-LE output daily surface
 temperatures on the atmosphere grid but not on the sea-ice grid, so surface temperatures from the daily atmosphere model were
 regridded onto the ice grid for all conductive heat flux calculations. Comparisons between these calculations using regridded
 atmospheric surface temperatures and those from the CICE model component were compared in CESM1-TS (which output
 40 both) confirmed that using re-gridded atmospheric output did not substantially change the results.

Mean Arctic ocean differences between model output (CESM1-CICE) conductive heat fluxes and those calculated using grid-
 cell mean values of ice and snow thicknesses (MNthick) tend to be an order of magnitude larger than those calculated using
 heterogeneous ice and snow fields (“0layer-ITD”; Supplemental Fig. 2) for most winter months. In the months of January and
 45 February for each of the time slices, 0layer-ITD estimates lie within 0.6 W/m² (or 2.1%) from the CESM1-CICE calculations
 (Supplemental Table 2), whereas those using the grid-cell means are less than the model outputs by 5.6-9.5 0.6 W/m² (or 15.5-
 39.1%). Conductive heat fluxes increase in all calculations as sea ice thins, despite decreases in temperature gradients, and the
 errors from the model output increase/decrease for the 0-layer estimates using ITD/grid-cell mean sea ice and snow thicknesses.

References

50 DuVivier, A. K., DeRepentigny, P., Holland, M. M., Webster, W., Kay, J. E., and Perovich, D.: Going with the floe: tracking
 CESM Large Ensemble sea ice in the Arctic provides context for ship-based observations. *The Cryosphere*, 14(4), 1259–1271.
<https://doi.org/10.5194/tc-14-1259-2020>, 2020.

Hurrell, J. W., Hack, J. J., Shea, D., Caron, J. M., and Rosinski, J.: A new sea surface temperature and sea ice boundary dataset
 55 for the Community Atmosphere Model. *Journal of Climate*, 21, 5145–5153, 2008.

Simpson, I. R., Bacmeister, J., Neale, R. B., Hannay, C., Gettelman, A., Garcia, R. R., and coauthors: An evaluation of the
 large-scale atmospheric circulation and its variability in CESM2 and other CMIP models. *Journal of Geophysical Research:*
Atmospheres, 125, e2020JD032835. <https://doi.org/10.1029/2020JD032835>, 2020.

Figure captions

Supplemental Figure 1. Changes in ensemble mean January net surface heat flux (netSHF; a-d) and surface temperatures (TS; e-h) for CESM2 PAMIP (a-c, e-g) and AMIP (d, h). PAMIP differences are from an 1850 pre-industrial control run where both SSTs and SICs are specified at 1850 levels. Differences from the PI are shown for PAMIP experiments with present-day
65 SSTs and SICs (pdSST-pdSIC; a,e); present-day SSTs and future SICs (“pdSST-futArcSIC; b, f), and future SSTs and SICs (futSST-futArcSIC; c, g). AMIP simulations are from a 10-member ensemble and differences shown are ensemble mean of the final decade (2005-2014) minus the first decade (1950-1959) of the simulations. The 98% SIC contour is shown in black.

Supplemental Figure 2. CESM1 two-year timeseries of area-averaged Arctic Ocean conductive heat fluxes from the model
70 output (CESM1-CICE; navy blue) and the Semtner 0-layer model calculations using daily sea ice and snow thicknesses from 5 discrete thickness categories (0layer-ITD; light blue) and using grid-cell mean sea ice and snow thicknesses (MNthick; medium blue). Differences from the model output are shown in dotted lines with scale on the right for both 0-layer model calculations (0layer-ITD in light blue, MNthick in medium blue). Ensemble means are shown in the solid lines, ensemble ranges in opaque polygons. Arctic Ocean region is shown in the map insert in the middle panel in Fig. 1.

75 **Supplemental Figure 3.** CESM1-LE February ensemble decadal mean (a-c) and decadal mean differences (d-i) in sea ice thickness (a, d, g), snow thicknesses (b, e, h) and effective snow thicknesses, $K_{\text{ratio}} * h_s$ (c, f, i). The 98% SIC for each decade is shown by the thick black contour. Stippled areas and dotted contour line indicate regions where mean/changes in effective snow thickness ($K_{\text{ratio}} * h_s$) account for 40% or more of the mean/changes in the total effective thickness ($h_{\text{eff}} = \text{SIT} + K_{\text{ratio}} * h_s$).

80 **Supplemental Figure 4.** Decadal mean differences between February conductive heat fluxes from the model output (CESM1-CICE) and those calculated using grid-cell mean thicknesses (MNthick) for the 2010s (a) and 2050s (b).

85 **Supplemental Table 1.** Conductive heat fluxes (Fcond) for example sea ice thicknesses (SIT), snow thicknesses (h_s), and temperature gradients (ΔT).

SIT (m)	h _s (m)	ΔT (°K)	Fcond (W m ⁻²)
2.0	0.1	40.	30.
2.0	0.02	40.	37.5
2.0	0.1	20.	15.
2.0	0.02	20.	18.75
0.5	0.1	40.	68.57
0.5	0.02	40.	126.32
0.5	0.1	20.	34.29
0.5	0.02	20.	63.16

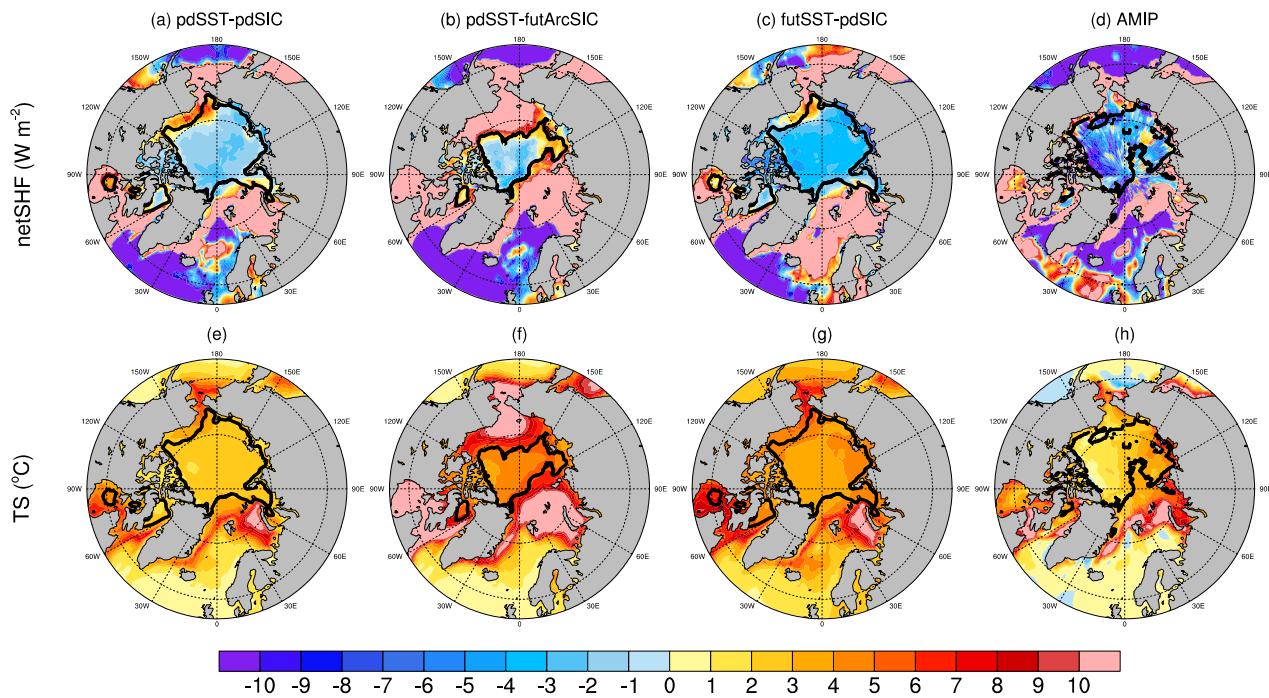
90 **Supplemental Table 2.** Ensemble mean differences between CESM1 monthly conductive heat fluxes (CESM1-CICE) and those calculated using the Semtner 0-layer model with sea ice and snow thicknesses from the 5 thickness categories (0layer-IDT) and from grid-cell mean sea ice and snow thicknesses (MNthick) for three time-slices.

method	CESM1-CICE - (0layer-IDT)						CESM1-CICE – (MNthick)					
year	1980-1981		2021-2022		2051-2052		1980-1981		2021-2022		2051-2052	
month	W m ⁻²	%	W m ⁻²	%	W m ⁻²	%	W m ⁻²	%	W m ⁻²	%	W m ⁻²	%
10 (Oct)	-1.9	-8.3	0.7	3.4	0.6	11.4	-12.7	-54.3	-7.6	-40.1	-1.7	-31.6
11 (Nov)	-1.3	-4.4	1.3	4.0	3.7	17.6	-12.8	-43.4	-7.6	-22.8	0.6	2.9
12 (Dec)	-0.6	-2.3	-0.0	-0.1	2.3	6.1	-11.2	-40.8	-8.9	-25.3	-2.5	-6.7
13 (Jan)	-0.2	-0.7	0.3	1.0	0.5	1.3	-9.5	-39.1	-8.2	-27.1	-5.6	-15.5
14 (Feb)	0.4	1.9	0.5	1.8	0.6	2.1	-8.4	-38.1	-7.9	-29.2	-6.0	-20.0
15 (Mar)	0.9	5.1	1.	4.7	0.9	3.7	-6.9	-37.4	-6.5	-29.8	-5.8	-24.1

CESM2 (ens mean) JAN

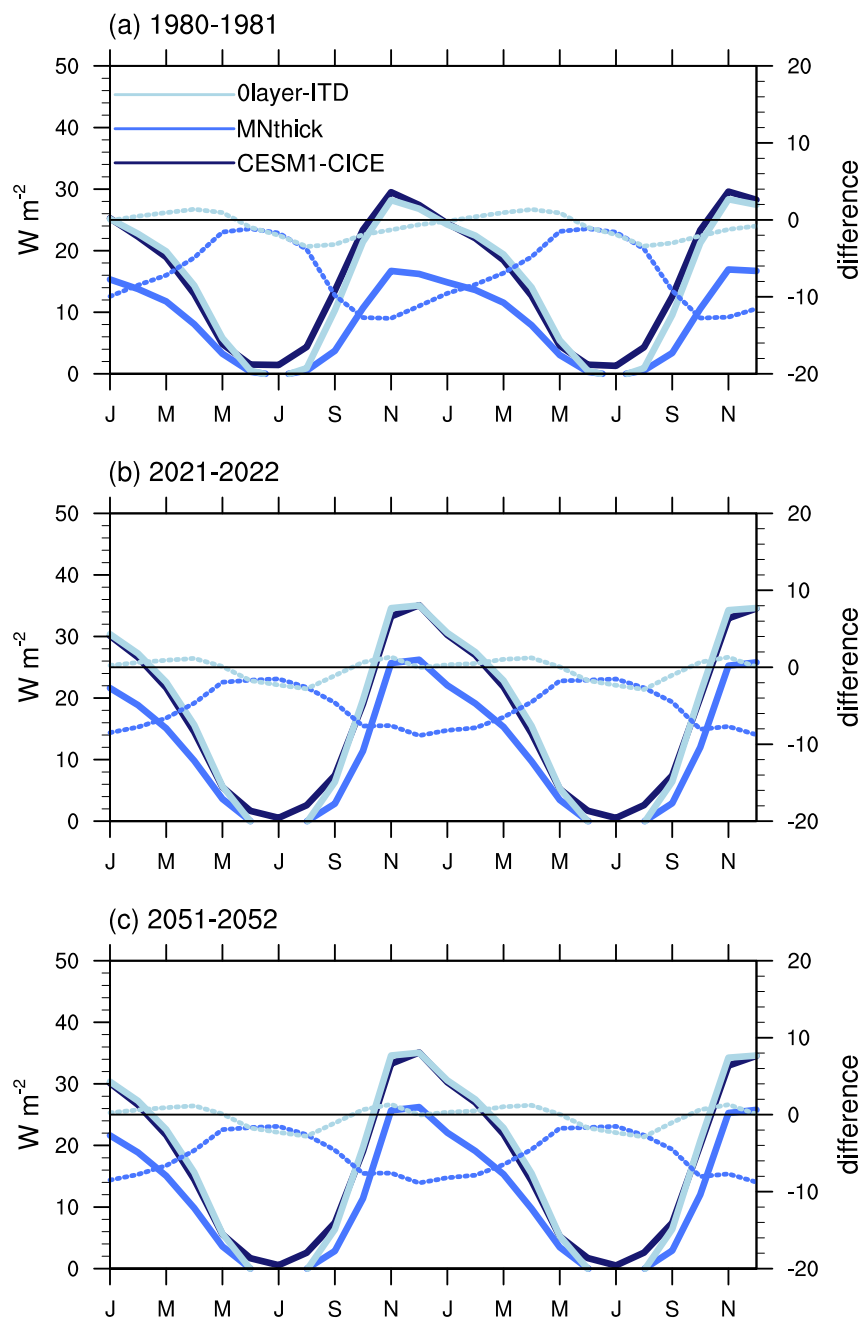
PAMIP (changes from PI)

AMIP ((2005-2014) - (1950-1959))



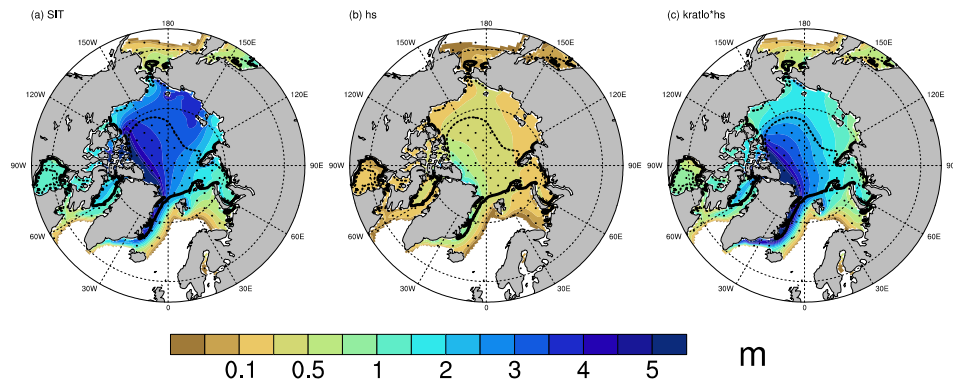
Supplemental Figure 1

Arctic Ocean conductive heat flux

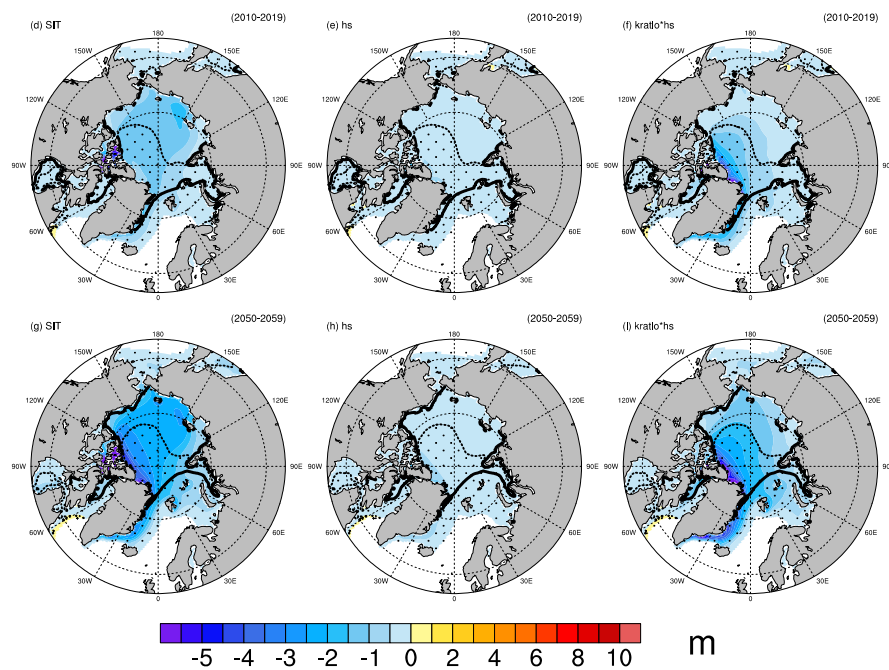


Supplemental Figure 2

FEB (1950-1959)



change from (1950-1959)



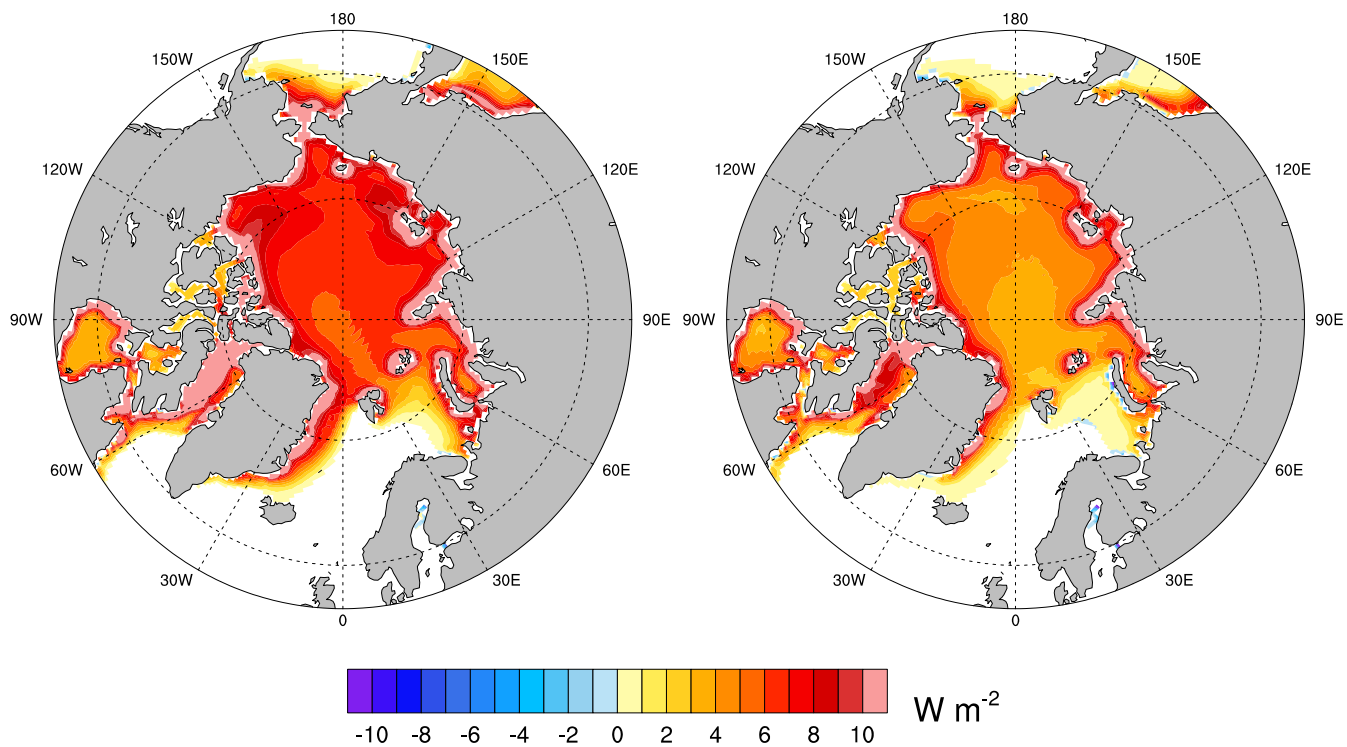
Supplemental Figure 3

Conductive heat flux

(CESM1-CICE) - (MNthick)

(a) (2010-2019)

(b) (2050-2059)



Supplemental Figure 4